Chapter 4
FILLER CHARACTERIZATION AND DESIGN OF ASPHALT MASTICS

4.1 Prologue

The highway sector is in search of pavement materials that could reduce not only the replenishment of natural resources but also improves the functioning of asphalt pavements. The utilization of waste in the highway sector is an increasing trend owing to the modernization of the construction industry and sustainable government policies. It is a high potential sector for highway researchers with the aim of cleaner manufacturing as well as viable development.

4.2 Fillers

The filler, which is the finest proportion of the asphalt mixtures, greatly contributes to the behavior of mastics and mixes. This study focuses on sustainable development by utilizing different types of wastes as a replacement for mineral filler in asphalt mastics as well as asphalt mixtures. To accomplish this, waste fillers from different sectors, such as industrial waste (red mud & quartz), dimension stone waste (marble dust & limestone), and quarry waste (granite & basalt), were used as mineral fillers (refer to Figure 4.1). The location of the parent sources of all the fillers used in this study is shown in Figure 4.2. The detailed description of all the fillers used in this study is presented below:

(a)

(b)

(c)

(d)

(e)

(f)

Figure 4.1 Industrial waste (a) RM (b) QZ, Dimensional stone waste (c) MD (d) LS, and Quarry waste (e) GR (f) BA

4.2.1 Red mud

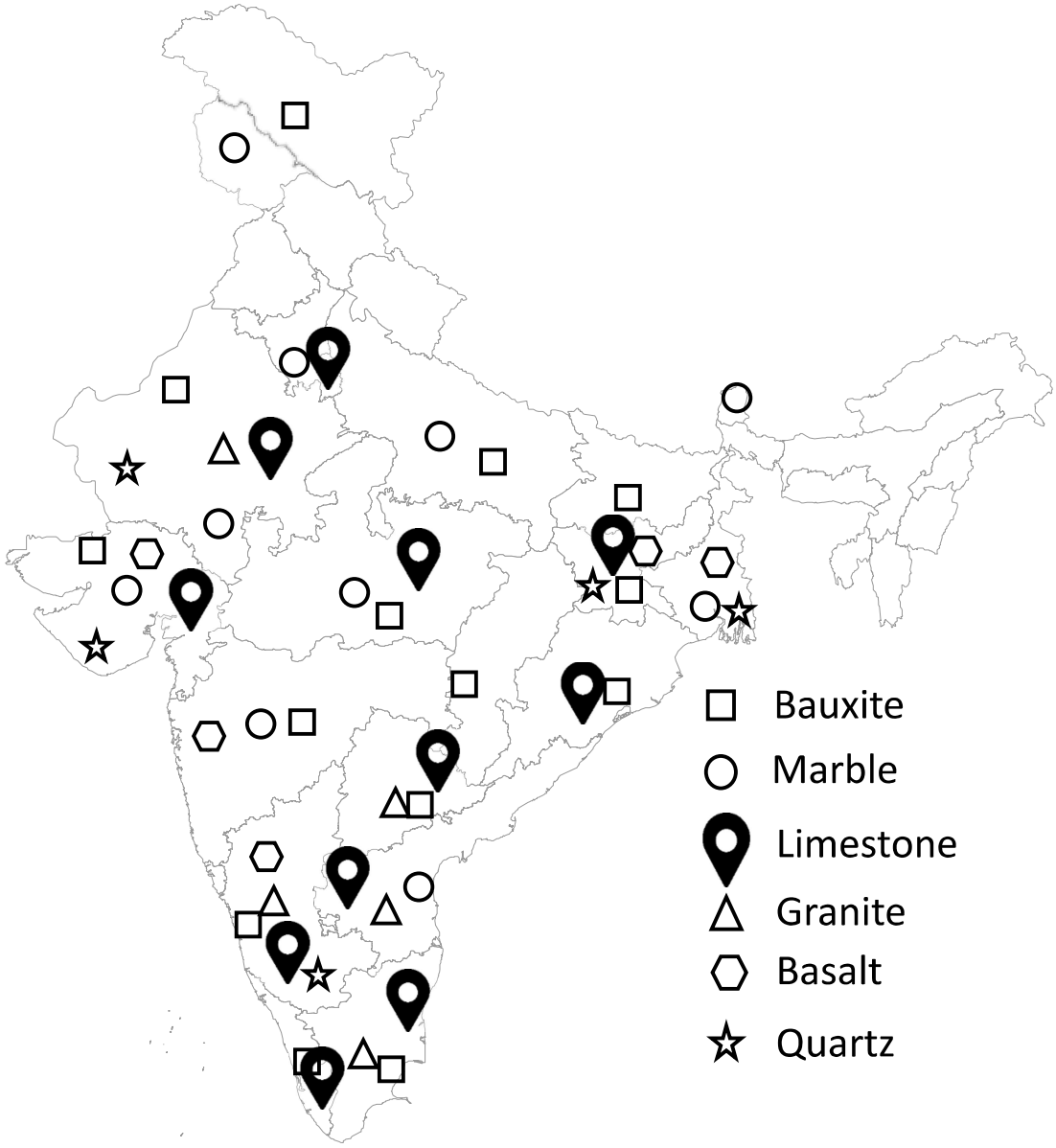

Figure 4.2 Sources of the parent rocks from where the fillers are derived [248–254]

Red Mud, also known as bauxite tailings, is a by-product generated during the production of alumina from bauxite ore through Bayer's process, which is then further processed to finally obtain the aluminium metal [255]. The process includes washing, crushing, and dissolving

bauxite ore in sodium hydroxide solution at relatively high pressure and temperature to form sodium aluminate [256,257]. The obtained sodium aluminate is then subjected to filtration and calcination to produce alumina, and the residue is known as red mud. The generation of RM is approximately 0.6-2.5 times the total alumina production [258]. The global industries are generating red mud at the rate of 145 million tonnes per year,f which India is contributing 4 million tonnes [259]. Approximately 55 to 75 billion tonnes of bauxite reserves are currently on the earth, of which 18% are in Asia [255].

The RM is a highly alkaline and voluminous industrial waste with a primary component of metal oxides (Fe, Al, and Ti) and radioactive elements [260,261]. It is very fine and difficult to compact on land or settle in the water, hence discharged in the surroundings. The generated huge volumes and the toxicity of bauxite tailings cause severe environmental pollution hazards and need a search to be tackled efficiently [262]. Due to these unforeseen circumstances, the utilization of red mud is imminent. The past applications of utilizing red mud include ceramics [263], special types of cement [264], embankments [265], bricks [266], clay liners [14], etc. but its use in the pavement industry is seldom. To address all these problems in a single stroke, it can be utilized as a filler material in hot mix asphalt to construct flexible pavements.

4.2.2 Quartz

It is a hard crystalline mineral with the primary composition of silica and is the most prevalent mineral in the crust of Earth after feldspar. It is a major constituent in all types of rocks, i.e., igneous, sedimentary, and metamorphic rocks [268]. Quartz is also an industrial waste generated while manufacturing glass, ceramics, and foundry molds in metal casting [269]. During glass production, the crushing of quartz stone, followed by wet sieving, produces quartz sludge containing very fine quartz particles. These particles, although non-hazardous but may cause several other nuisances such as air contamination, hindrance in the vegetation, land occupation for waste disposal, etc. [270]. In the foundry industry, quartz sand is reused several

times in producing mineral sand molds mainly used to cast metal parts. The repeated usage contaminates the quartz, which is discarded in the form of waste [271]. The waste quartz found its application in different fields, such as concrete production, soil stabilization, retaining walls, etc. [272].

4.2.3 Marble dust

The waste generation during marble processing can be as high as 30% [273]. The dumping of marble dust can cause several nuisances, such as air pollution attributed to very fine particle size, land pollution caused by the blocking of soil pores, and clogged water drains and aquifers [274] The dried slurry of marble dust is fine in size, with 90% particles finer than 200 microns [275] and hence has the potential to be used as a filler in asphalt concrete mixes.

4.2.4 Limestone

The limestone has been found in many countries, including India. It is cheaper than marble and attains similar polish marble; hence, it has a higher market demand [276]. The mined limestone requires finishing like cutting, sawing, and polishing to obtain the desired smoothness, producing a huge quantity of fine solid waste known as limestone dust. As an approximation, 60% of the mined limestone ends up as waste and hence requires proper disposal [80,277,278].

4.2.5 Granite

Granite aggregates are widely used in the construction of flexible pavements. The granite in the form of dust is generated from the quarries during the processing of granite rocks to produce aggregates which are discarded as waste because of no commercial value. Granite dust is a high volume waste that can fill the land space in a shorter time duration and hence can be effectively used as a filler in pavement construction.

4.2.6 Basalt

Basalt aggregates have been extensively used in asphalt mixtures and road foundations. The basalt dust is generated during the production of high-quality aggregates from basalt rocks [279]. The powdered form of basalt is separated from the aggregates on the production line, and heaps are formed. Although it is natural and inert, the small-sized fine particles can cause severe respiratory hazards confirmed by ecotoxicological tests [280]. The remedy for the utilization of large quantity basalt waste has been investigated for a long period. It is used in the field of agriculture since basalt rocks serve as a substrate for high quality fertile soils [279]. Another application of fine grained basalt dust is in the ceramics industry, where it is the constituent of dark colored ceramic glazes in small quantities. But, bulk utilization can be achieved by using it in the road sector. Owing to its non-toxicity, temperature resistivity, and high chemical stability [281], fine basalt dust can be used as the filler in the asphalt mixture, preventing the replenishment of natural rocks and providing an effective solution for waste disposal.

4.3 Characterization of Fillers

The filler is an integral part of the asphalt mixture, which primarily affects the performance of asphalt mastic, asphalt mixtures, and, eventually, the pavement [282]. Despite the plethora of research emphasizing the dictating role of filler properties on the performance of asphalt mixtures, no detailed specifications about the filler properties except the filler-binder ratio and material gradings have been mentioned in most of the guidelines [283]. Superpave design specifications recommend the filler-binder ratio in the range of 0.6-1.2. MoRTH, India guidelines have only considered the gradation and plasticity index as the parameters to screen the fillers. These parameters are insufficient to describe the effect of filler in the mastics as well

as the mixes. Therefore, the fillers are characterized by the wide range of physical, morphological, and chemical tests in this study as described below:

4.3.1 Particle Size Analysis (PSA)

The hydrometer analysis was used for the fillers' particle size distribution (PSD) as per IS 2720-4 (1985) which involved relating the particle size with the specific gravity of the suspension containing filler, water, and deflocculating agent at the center of the hydrometer bulb. The hydrometer readings were taken at intervals of 0.5, 1, 2, 4, 8, 15, 30 minutes, and 1, 2, 4, 8, 12, and 24 hours respectively, as shown in Figure 4.3. Three corrections were applied to the measured hydrometer readings: meniscus, temperature, and dispersing agent corrections. The percentage fines can be calculated as follows:

$$\% \, Finer = \left(\frac{G}{G-1}\right)\frac{R}{W_{sample}} * 100 \tag{4.1}$$

The diameter of the particle is expressed as:

$$D = K * \sqrt{\frac{H_e}{t}} \tag{4.2}$$

and

$$K = \sqrt{\frac{18\eta}{G-1}} \tag{4.3}$$

Where G = specific gravity of the sample

R = corrected hydrometer reading

H_e = effective height

W_{sample} = weight of the sample

t = elapsed time

η = viscosity of water

The PSD is the qualitative process of determining the distribution of particles in the mineral filler. It can be quantified using a mathematical entity known as the fineness modulus (FM). It is a fineness parameter that represents the relative fineness of the materials and is calculated by dividing the sum of the percentages of filler coarser than 75, 50, 30, 20, 10, 5, 3, and 1 μm with 100. The smaller value of FM indicates the presence of finer particles in the filler.

Figure 4.4 presents the PSD obtained from the hydrometer test. It is observed that the BA has the coarsest particle size distribution (PSD), followed by MD and LS. On the other hand, the finest PSD corresponds to RM, followed by QZ and GR. These observations were also justified by the FM values given in Table 4.1, where BA and MD have higher FM, whereas lower values of FM belong to RM and QZ. The PSD curve shows that the relative difference in the fineness of RM and other fillers was very high compared to the difference among GR, BA, MD, and LS.

Figure 4.3 Hydrometer test

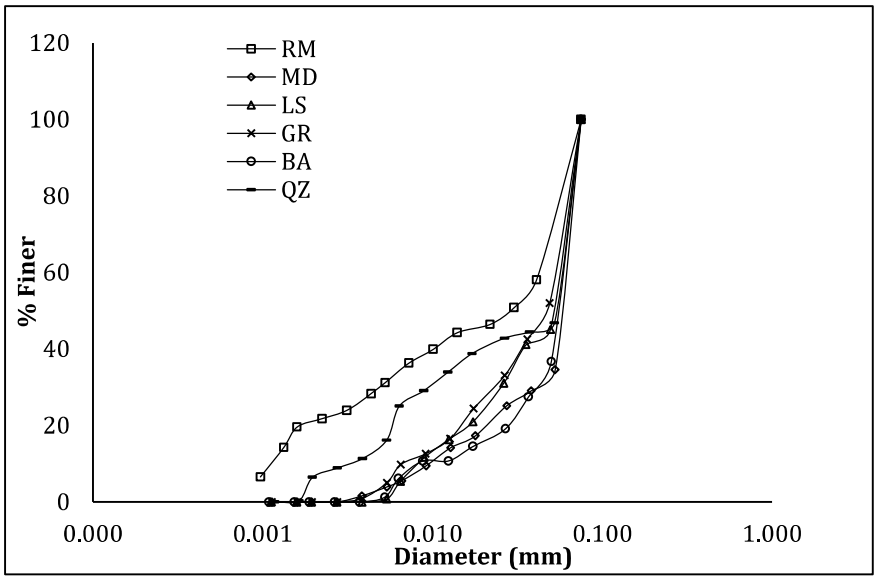

Figure 4.4 Particle size distribution

4.3.2 Rigden Voids

The void content in the well-compacted bed of fillers is known as Rigden voids. It is named after the researcher PJ Rigden who introduced this concept by showing a strong dependence on filler stiffening effect on the void content [284]. He conducted a series of experiments to study the influence of filler properties on the viscosity of asphalt mastics and introduced the concept of free and fixed asphalt [285]. The amount of asphalt binder required to fill the inter and intra granular voids in a dry compacted bed of fines/fillers is called fixed asphalt, whereas the excess binder is known as free asphalt. Hence, the free asphalt is responsible for providing workability and flowability to the mix and defines the consistency of the filled system. In a similar study, Heukelom [286] suggested that adding the binder in a lesser quantity than required to fill the voids will result in a dry and stiff mixture, whereas overfilling will impart excessive fluidity.

The Rigden voids are the function of geometrical characteristics of filler such as shape, size, texture, angularity, etc. [287]. The influence of fractional voids of filler on the performance of

asphalt mastics, as well as asphalt mixtures, has been extensively studied by many researchers [241,288,289].

The void content in the fillers compacted to maximum density can be determined using the Rigden voids apparatus as per BS 812. In this method, a small sample of oven dried sample was compacted by 25 blows of the hammer to achieve maximum compaction and form a compacted bed of fillers. The following equation calculates the voids in the compacted fines:

$$RV\ (\%) = \left(1 - \frac{G_b}{G_s}\right) \tag{4.4}$$

And

$$G_b = \left(\frac{M}{V}\right) \tag{4.5}$$

Where,

RV is the void content, or Rigden voids

G_b is the bulk specific gravity of the fines obtained by compaction,

G_s is the apparent specific gravity of fines

M is the mass of filler (g)

V is the volume, product of the cross-sectional area (cm^2) of the Rigden voids apparatus and the depth (cm) of the compacted filler bed.

Table 4.1 presents the properties of the fillers obtained by various physical, morphological, and chemical characterization tests. The RV of RM was found to be very high compared to the remaining fillers. It was approximately seven times the RV of BA, which signifies that the quantity of structured asphalt to fill the voids between the fillers can be very high, and a high OBC is expected with using RM as filler which is quite uneconomical in the mix design. The

least RV corresponds to BA, followed by MD. Interestingly, the trend in RV was exactly reversed in FM, which is quite logical because the finer PSD prevents the dense compaction of the filler bed by the compactor, due to which more space is available between the filler particles and hence results in higher voids.

Table 4.1 Physical properties of fillers

Filler	SSA (m^2/g)	SG	RV (%)	MBV (g/kg)	FM	D_{60}	D_{10}	FGC
RM	27.825	3.22	45.7	2.5	4.32	41	1.11	0.97
MD	1.208	2.75	12.1	3	6.06	50	10	0.80
LS	0.755	2.81	22.4	1.5	5.81	70	8.4	0.88
GR	2.436	2.74	27.6	2.5	5.7	60	7.2	0.88
BA	11.869	2.9	6.33	3	6.13	72	10.5	0.85
QZ	3.32	2.63	27.8	1	5.12	67	3.3	0.95

4.3.3 Methylene Blue Value (MBV)

The MBV test is a French method recommended by the International Slurry Seal Association (Technical Bulletin 145 of ISSA) [290] used to detect harmful and active clay minerals, especially from the Smectite or Montmorillonite group in the material. This clay has expansive nature in the presence of water which can cause significant damage to the pavement when present in the filler. The MBV test is considered a quick and accurate method [295] and is carried out as per EN 933-09.

Ten grams of filler was dissolved in 30 gm of distilled water in a beaker and shaked continuously, so the material gets dispersed in the water. After that, 1 gm of Methylene Blue (MB) dye was dissolved in sufficient distilled water to obtain 200 ml of the solution. Now, the MB solution was filled to the mark in the burette, and the valve was closed. Then, the valve was released slowly to titrate the MB solution in 0.5 ml aliquots into the filler suspension. After

each addition of MB solution, the spot test was carried out by placing a small drop on the filter paper with the help of a glass rod. If all the dye had been absorbed, a well-defined circle of MB stained dust surrounded by an outer ring of clear water was formed. With the addition of aliquots, the ring becomes slightly blue in color. After the successive additions, the end point was reached when a permanent light blue color was observed in the ring. Figure 4.5 shows the various steps involved in the MBV test procedure.

The MBV is reported in terms of grams of MB dye per kg of the material and is mathematically expressed as [291]:

$$MB = \frac{V_i}{M_i} * 10 \qquad (4.6)$$

Where,

M_i is the sample mass (in grams), and V_i is the total volume added (in ml)

(a)

(b)

(c)

(d)

Figure 4.5 Methylene blue value test

It is to be noted from Table 4.1 that the MBV of all the fillers was lower than the threshold value of 10 g/kg, which implies that the amount of harmful clay is within the safe permissible limits for all the fillers and hence they can be used in the asphalt mix as far as swelling characteristics are considered.

4.3.4 X-Ray Diffraction (XRD) Analysis

The intensity plot of the sample with respect to the deflection angle is known as an X-ray diffraction pattern or X-ray diffractogram. An X-ray diffractometer has three basic elements: a sample holder, an X-ray tube, and an X-ray detector (Figure 4.6).

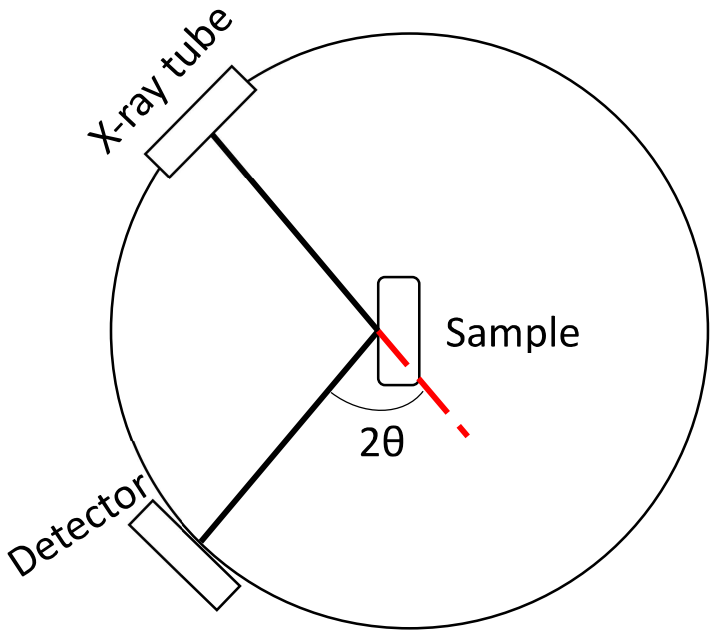

Figure 4.6 X-ray diffraction

The Rigaku benchtop X-Ray Diffractometer with Cu-Kα radiation was used in the study (Figure 4.7). The value of 2θ varied from 5° to 70° with a scan rate of 5° per minute. The wavelength of 1.5406 Å was employed to determine the mineralogical composition of the fillers.

(a)

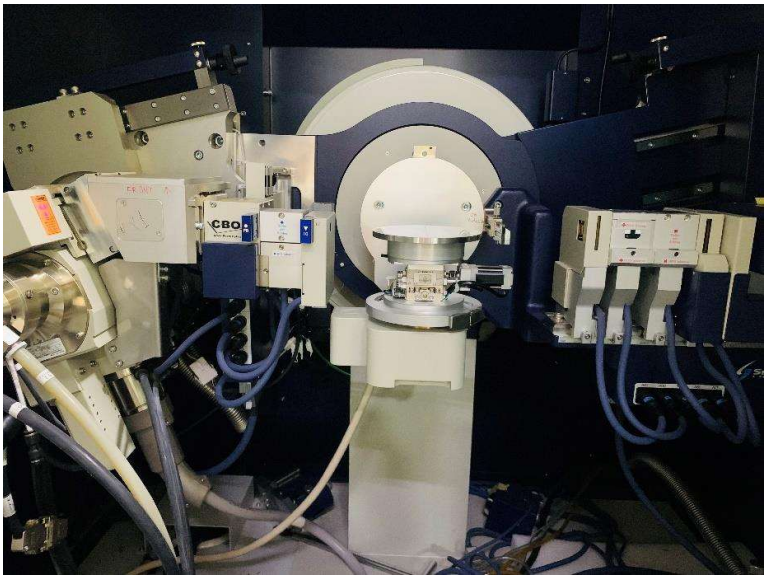

(b)

Figure 4.7 X-ray diffractometer

The X-ray diffractograms of the studied fillers are shown in Figure 4.8. Silica in the form of quartz has been found in the majority of the fillers in varying quantities. Calcite is another compound that was found in many of the aforementioned fillers. The RM contained oxides of Iron and Aluminium as Hematite and Kaolinite, respectively. They are believed to be responsible for the high-temperature performance and high stability; therefore, they can be a potential filler for rut-resistant mixes. The diffractograms, along with quartz, noted the presence of CaCO3 in LS in different crystalline phases like Calcite and Aragonite. MD is the calcite based filler with some amount of dolomite in it. Calcite and Dolomite are the minerals that provide good adhesion with bitumen [79,292] therefore, they can be used as a filler in the bituminous mixes to be laid in moisture-susceptible areas. The predominant mineral found in Granite was Quartz. Petersen et al. [293] stated that asphalt's acidic functionalities are readily adsorbed onto the aggregate adsorption sites. SiO_2 is grouped into the acid-insoluble category; therefore, quartz-rich fillers may find difficulty in asphalt adsorption, resulting in weak adhesion [294]. The predominant minerals observed in Basalt were Anorthite which are calcium end members of the plagioclase feldspar mineral series, while pyroxenes were present in a small amount.

The predominant minerals in the various fillers have been presented in Table 4.2. To quantify the XRD data concerning the presence of silicate, the total intensity was calculated from the diffractograms. The calculated values, in thousands, were found to be 33, 12, 27, 94, and 242 for *RM*, *MD*, *LS*, *GR,* and *QZ,* respectively. An attempt was made to correlate the intensity counts with various physical properties. It was found that the counts, excluding the data of *RM*, correlated well with the values of *FM* (R^2= 0.96), *SG* (R^2= 0.87), D_{60} (R^2=0.97), and *FGC* (R^2=0.77). The presence of RM results in a poor correlation between the physical properties and silicate intensity. This is attributed to the complexity associated with the characterization of Bauxite residue compared to other fillers. Cheng et al. [295] stated that the use of *XRD* for

the quantification of mineralogical characteristics of Diatomite produces complicated results. A similar nodus has been noted in this study due to the presence of analogous minerals in RM.

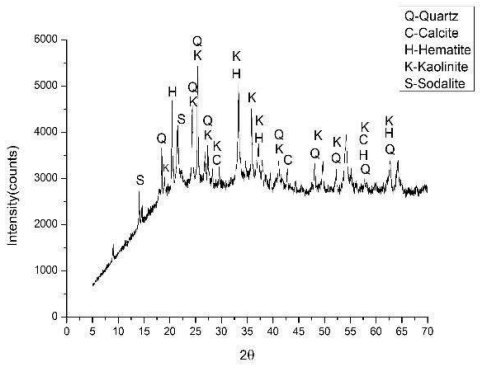

(a)

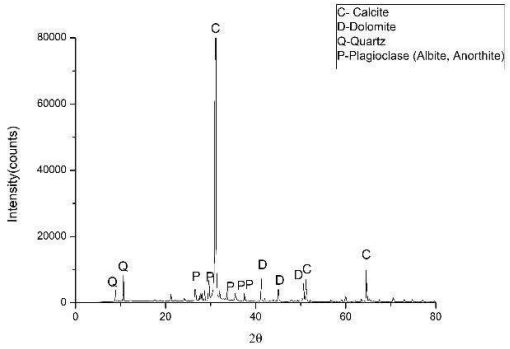

(b)

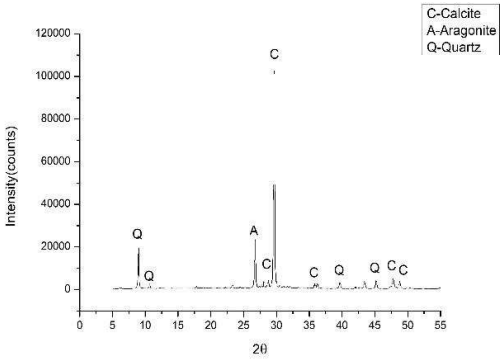

(c)

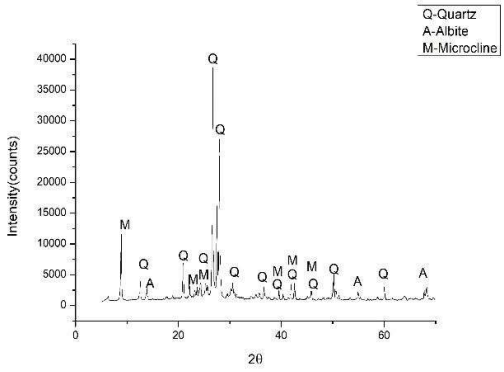

(d)

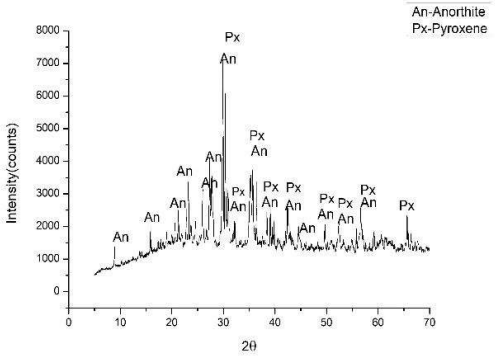

(e)

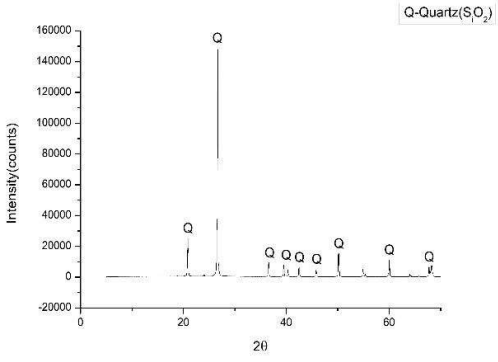

(f)

Figure 4.8 XRD patterns of (a) RM (b) MD (c) LS (d) GR (e) BA (f) QZ

Table 4.2 Predominant minerals in different fillers

	Hematite	Aragonite	Anorthite	Calcite	Pyroxene	Albite	Kaolinite	Quartz	Dolomite	Plagioclase
RM	✓	•		✓			✓	✓		
MD				✓				✓	✓	✓
LS		✓		✓				✓		
GR		•		•		✓		✓		
BA			✓		✓					
QZ								✓		

4.3.5 Scanning Electron microscope (SEM) Image Analysis

The surface morphology of the fillers affects the bond between the fillers and the binder. The conventional optical microscope can be magnified up to 1000 times only, which is not sufficient to study the surface characteristics of the materials (aggregate, filler, etc.). It can be achieved by decreasing the wavelength of imaging radiation as with SEM (Figure 4.9). The typical wavelength of the imaging radiation lies between 0.0009-0.027 nm for the electron microscope; hence a higher resolution can be achieved (as high as 10^6X) [296]. In addition to surface morphology, crystalline structure and electrical behavior assessment are the added advantages [296]. The SEM images of all the fillers are shown in Figure 4.10 at a magnification of 4.5 KX.

It is observed that the texture and shape varied from particle to particle within the same filler sample. The surface texture of RM was completely different from those of other fillers due to the presence of agglomeration at many places. The agglomeration in the RM has also been reported in previous studies [255]. It is clear from the Figure that the RM particles tend to stick to one another, due to which it is possible that the distribution of RM inside the mastic is not uniform. This may lead to ambiguous results depending on the part from which the sample is

taken from the mastic for the testing. Also, the particle shape was roughly on a rounder side. MD & LS have an almost similar type of grain shape and texture, flat surfaces with pointed edges. The flaky appearance in the surface texture of both fillers has also been seen in the SEM images. However, the surface of MD particles was quite smooth, whereas LS had slightly rough texture particles. This may result in better filler-binder bonding than the round-shaped RM particles. The plate or sheet like structure with the presence of agglomeration was observed in GR but to a lesser extent as compared to RM. The surface was rough due to the sticking of fine particles on the larger particles. BA had very large particles with round edges and a surface texture varying from slightly smooth to rough. QZ has the smoothest texture among all the fillers and has very sharp and pointed edges. The particles were elongated and in the form of laminated sheets.

Figure 4.9 Scanning electron microscope

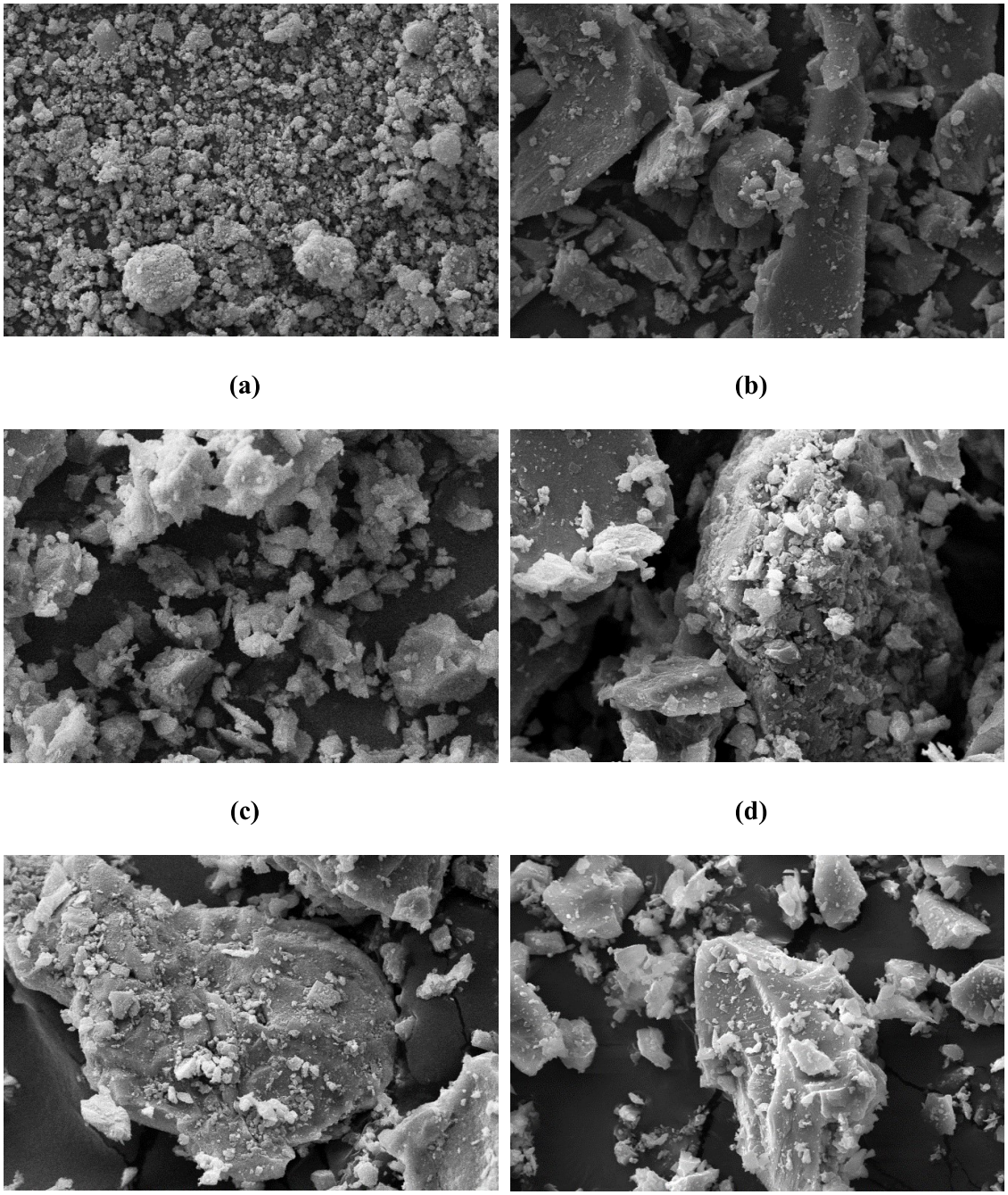

(a) **(b)**

(c) **(d)**

(e) **(f)**

Figure 4.10 SEM images of (a) RM (b) MD (c) LS (d) GR (e) BA (f) QZ at 4.5 KX magnification level

4.3.6 Specific Surface Area (SSA)

The surface area includes the external surface of the solid as well as the internal surface of accessible macro and mesopores. The most common method for the evaluation of the surface area of the powder materials is Brunauer, Emmett, and Teller (BET) technique. This method consists of a probe molecule (nitrogen gas generally) exposed to a solid under investigation at 77 K (liquid nitrogen conditions). The cross-sectional area of the probe molecule (taken as 16.2 $Å^2$ in the case of nitrogen) and the measured monolayer capacity is taken as input for determining surface area [297]. The amount of adsorptive gas required to cover the solid's external solid surface and internal pore surfaces is calculated. The calculated amount is dependent on the adsorption isotherm using the BET equation expressed as [43]:

$$\frac{p}{n^a(p^o - p)} = \frac{1}{{n^a}_m} + \frac{(C-1)}{{n^a}_m}.\frac{p}{p_o} \tag{4.7}$$

Where n^a is the amount adsorbed at the relative pressure p/p_o, n^a_m is the monolayer capacity, and C is a constant, which is dependent on the isotherm shape

A linear relation can be obtained by plotting $p/n^a(p^o\text{-}p)$ vs p/p^o known as BET plot to obtain n^a_m. Finally, the BET surface area (A) can be calculated by the average area, a_m (molecular cross-sectional area) occupied by each adsorbed molecule in the complete monolayer [298]:

$$A(BET) = {n^a}_m.L.a_m \tag{4.8}$$

Where L is the Avogadro constant.

(a)

(b)

Figure 4.11 BET testing apparatus

The SSA of the fillers was determined with the BET apparatus (Figure 4.11) as per ASTM E986-04. The SSA of RM was found to be the highest, followed by BA. This was, in fact, very interesting because despite having the coarsest PSD, BA has a higher SSA. It is a common misconception that the finer PSD corresponds to higher SSA, observed many times but not universal, as evident in this study. The PSD represents the proportion of the filler, which is finer than a certain size, but it does not quantify the exact fineness. For example, 43% of QZ particles were finer than 27 microns, but the exact fineness was not known. Moreover, the FM, a mathematical parameter to quantify the fineness, only represents the average fineness of a wide range of particles with variable particle sizes. On the other hand, SSA represents the surface area of particles in 1 gm of the sample, which is a very less quantity and hence a more precise parameter for the fineness. Hence, the FM and SSA can be related to each other, but they were not exact indicators of each other. This is also evident from the average correlation (R^2=0.68) between FM and SSA in Table 4.3.

4.3.7 Specific Gravity

Specific gravity or relative density is defined as the ratio of a material's density (mass per unit volume) to the density of a standard material. The standard material is generally considered water, whose density is unity; therefore, specific gravity and density are mostly used interchangeably. The filler particles' specific gravity was evaluated using the Pycnometer method as per ASTM D854.

The RM was found to be the heaviest filler, as evident from the highest SG. This can be attributed to the presence of hematite in it. On the other hand, QZ was the lightest filler, whereas MD and GR have identical SG. The obtained range of SG varies to a high extent ranging from 2.63 (QZ) to 3.22 (RM). Such a wide range of the SG of the fillers demands the addition of filler on a volume basis rather than by weight. The addition of filler by weight can result in

unequal distribution of filler particles within the asphalt binder. For example, the higher SG filler will occupy lesser space, whereas the lighter filler will occupy a larger space within the asphalt matrix for the same weight. Due to this, the filler stiffening effect will primarily be dependent on the SG of the filler rather than on the fundamental filler characteristics like shape, size, RV, SSA, etc. Hence, the fillers are added in equal volumetric concentrations in this study to produce homogenous asphalt mastics.

4.3.8 Filler Grain Coefficient (FGC)

The two most common parameters used for the quantification of particle distribution in any suspended mass are D_{60} and D_{10}. The subscript represents the percentage of the filler mass finer than the particular diameter. So, D_{60} is the particle diameter corresponding to which 60% of the filler mass is finer, whereas D_{10} is the diameter that represents the 10% finer particles. The lower value of D_{60} signifies the finer grain sizes, whereas the higher difference between D_{60} and D_{10} signifies a greater bandwidth of particles within this range and hence the well graded distribution of filler particles. A new mathematical parameter called FGC has been introduced in this study to accurately quantify the particle distribution in the system expressed as follows:

$$FGC = \frac{D_{60} - D_{10}}{D_{60}} \tag{4.9}$$

It is apparent from Equation (4.9) that the higher value of FGC represents the well graded and finer distribution of particles. The RM and QZ were found to have the highest FGC and hence represent the well graded nature of fillers. The PSD curves also justified this observation.

4.4 Correlation Analysis

Table 4.3 shows the correlation matrix for all the physical properties of the fillers [77,287,299,300]. The correlations were established by using a linear fit between the variables. MBV, being a chemical test, was not included in the correlation Table of the physical

properties. It is observed that strong correlations have been observed between FM, FGC, D_{10}, and RV. Previous research has shown mixed correlations between FM and RV. Faheem and Bahia [299] have observed an appreciable correlation between FM and RV, whereas other researchers reported a poor correlation between the same [77,301]. The aforementioned correlation matrix portrays a negative correlation of RV with FM, which was also confirmed by Wang et al. [287].

The results showed that the correlation matrix could only provide an idea about the interrelation between the parameters. However, the influence of the different filler properties on the fatigue behavior of asphalt mastics can be justified only by the rheological testing and analysis of the mastics under different loading conditions, which will be discussed in the later chapters. For example, FM showed a strong correlation with all the measured filler parameters. This indicates that the chosen set of diverse fillers can be used as an indicator for characterizing the physical behavior of fillers but cannot be attributed as the filler property affecting the performance of mastics without actual testing.

Table 4.3 Correlation matrix for various properties of fillers

Correlation	FM	SG	D_{60}	D_{10}	FGC	RV	SSA
FM	1						
SG	-0.58	1					
D_{60}	0.59	-0.58	1				
D_{10}	0.98	-0.41	0.48	1			
FGC	-0.91	0.40	-0.20	-0.94	1		
RV	-0.94	0.50	-0.58	-0.93	0.85	1	
SSA	0.55	0.61	0.51	0.54	-0.49	-0.90	1

4.5 Asphalt Binder

Two types of binders, one unmodified binder (VG-30) and another polymer modified binder (PMB-40) are used in the study for the asphalt mastics and mixtures preparation. The consistency of the binders is determined through different tests as stated in Table 4.4 and Table 4.5.

Table 4.4 Physical properties of asphalt binder (VG-30)

Property	Value	Limit (IS 73:2013)	Reference
Penetration, dmm	62	45 (min.)	IS: 1203
Softening Point, °C	48	47 (min.)	IS: 1205
Viscosity at 60 °C, Poises	2704	2400-3600	IS: 1206 (II)
High Temperature PG	PG 70-XX	-	ASTM D 6373
Continuous Upper PG, °C	74.30	-	ASTM D 6373

Table 4.5 Physical properties of asphalt binder (PMB-40)

Property	Value	Limit (IS 15462:2004)	Reference
Penetration, dmm	45	30-50	IS: 1203
Softening Point, °C	67	60 (min.)	IS: 1205
Elastic recovery, 15 °C, %	78	70 (min.)	IS: 15462
High Temperature PG	PG 76-XX	-	ASTM D 6373
Continuous Upper PG, °C	79.80	-	ASTM D 6373

4.6 Preparation of Asphalt Mastics

A simple procedure was adopted to prepare asphalt mastics in the laboratory. The filler was accurately weighed on the measuring scale corresponding to the F-B ratio, followed by temperature controlled heating at 180 °C for 1 hour. The required amount of asphalt binder was also heated at the same temperature for 10 minutes. The filler and the binder were then mixed in the can and agitated continuously with the help of a manually operated mixer for 10 minutes. The mixing was done to ensure uniform distribution of mineral fillers inside the binder matrix. The can was then placed in the deep freezer immediately so that the filler particles did not settle at the bottom.

4.7 Aging

The prepared mastic samples were subjected to short term aging followed by long term aging. Conventionally, the laboratory uses a rolling thin film oven and pressure aging vessel for short-term and long-term aging of asphalt binders/mastic. In this study, the aging of the mastic samples was done by utilizing the Universal Simple Ageing Test (USAT) protocol proposed by WRI [245]. The USAT method has the merit of using the common draft oven to age the asphalt samples [302]. The aging process involves spreading the mastic samples in the flat plate to a very thin layer thickness with the help of a spatula. The plate was then kept in the draft oven for a period of 50 minutes at a temperature 150^{o}C for STA. The LTA was carried out on the STA samples by placing them in the oven for a period of 40 hours at a temperature of 100^{o}C (Figure 4.12). In the development of the USAT, the authors showed that the newly developed aging test method directly simulates the STA and LTA by RTFOT and PAV tests, respectively, in terms of aging temperature, pressure, and aging time. This method has also been adopted in several scholarly articles [303–305].

(a)

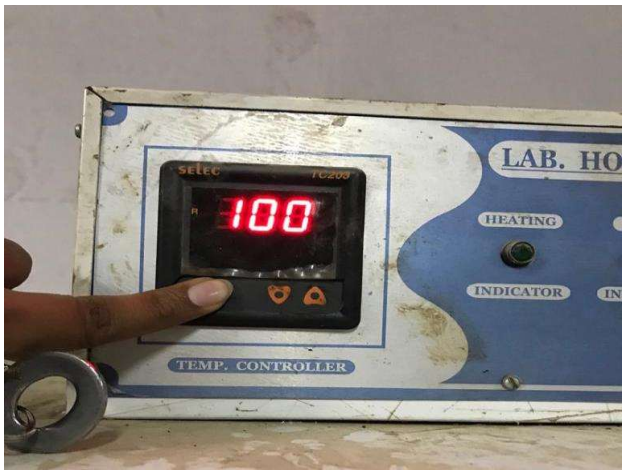

(b)

(c)

Figure 4.12 (a) Short Term Aging (b) Long Term Aging (c) Aging Plates

4.8 Comparison with SHRP LVE limits

The rheological behavior of the asphalt binders and asphalt mastics is generally determined within the LVE limit or strain (γ_{LVE}). The result representation techniques, such as master curves, cole-cole plots, black diagrams, etc., can be implied only within the LVE limits due to the TTSP. Therefore, many research articles have highlighted the importance of linearity limits of asphalt binders for both unmodified and modified binders [3,306–308]. In addition to that, the researchers also investigated the linearity limits of bituminous binders under different

loading conditions. The LVE [197,309] strain was evaluated from the amplitude sweep test in this study using the DSR.

The SHRP study on the LVE limits showed that the shear stress or shear strain linearity limit of the asphalt binders is dependent on the complex modulus of the binder defined by the following equations [310]:

$$\gamma_{LVE} = \frac{12}{|G^*|^{0.29}} \tag{4.10}$$

$$\tau_{LVE} = 0.12 \times |G^*|^{0.71} \tag{4.11}$$

Where,

γ_{LVE} is the shear strain (%),τ_{LVE} is the shear stress (kPa), and $|G^*|$ is the complex modulus (kPa).

Equations (4.10) and (4.11) show the SHRP relationships to determine the LVE stress/strain limits. However, no such relationship has been provided in any document to calculate the LVE stress/strain of asphalt mastics. An attempt has been made in this study to find out the relation between linear viscoelastic complex modulus ($|G^*|_{LVE}$) and LVE strain for the asphalt mastics using both VG binder and PMB. A similar relationship was also determined using SHRP binder criteria to check the applicability, as shown in Figure 4.13.

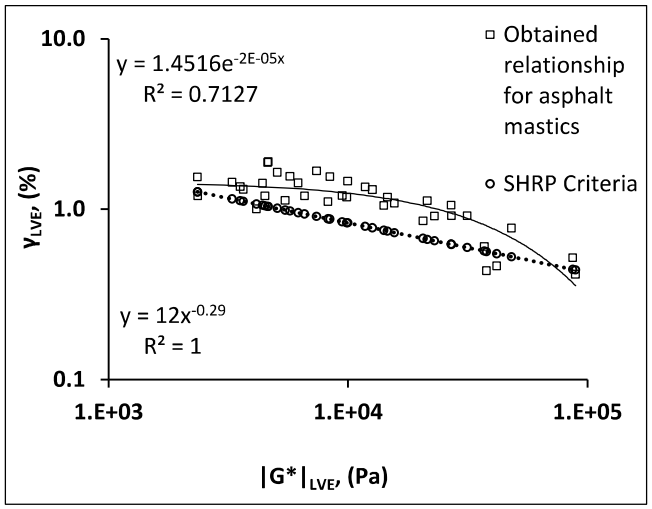

(a)

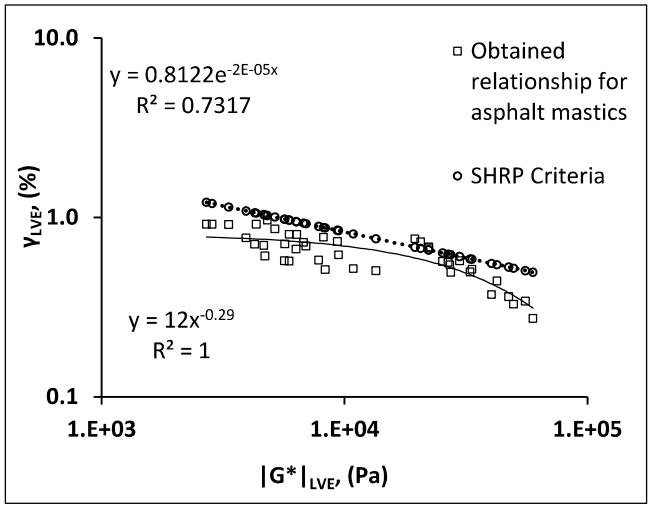

(b)

Figure 4.13 Relationship between LVEM and LVE strain for asphalt mastics in case of (a) VG-30 binder and (b) polymer modified binder

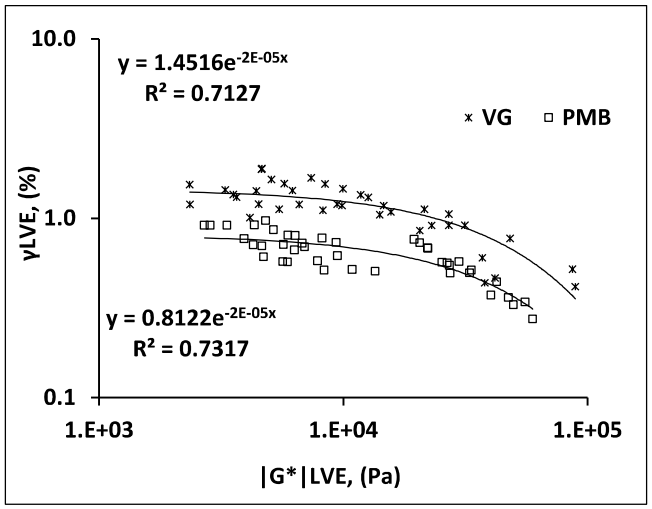

Figure 4.14 Comparison between LVE limits of asphalt mastics for VG binder and PMB

The illustrated relationship in Figure 4.13 is independent of the filler type, temperature, and filler content and can be used for the LVE strain calculation in DMA experimentation and analysis of asphalt mastics. It is observed that the LVE strains obtained from the SHRP criteria were on the conservative side with VG binder, whereas opposite trends were observed with PMB. In addition, the relationship between $|G^*|_{LVE}$ and LVE strain follows an exponential model compared to the SHRP power law criteria. Hence, the SHRP binder criteria are not applicable to the results of asphalt mastics. Figure 4.14 shows the LVE limits for both binders in which the LVE limits of PMB samples were found to be lower than that of VG counterparts. These observations are in accordance with the results published in previous literature [311].

4.9 Summary

This study engaged fillers from different sectors, such as red mud and quartz from industrial wastes, marble dust and limestone from dimensional stone waste, and granite and basalt from quarry waste. The gradation and plasticity index suggested by MoRTH guidelines are not sufficient to accurately characterize the properties of the fillers; hence, a wide range of tests were conducted. The chosen fillers displayed a wide range of properties which justified that

these properties cannot be ignored, and detailed characterization of fillers is necessary and should be considered in the asphalt mix design. The correlation analysis showed that a common parameter having a strong correlation with all the measured filler properties could be used as the indicator for filler characterization. The SHRP criteria for determining the LVE limits of asphalt binders were not applicable in the case of asphalt mastic.